


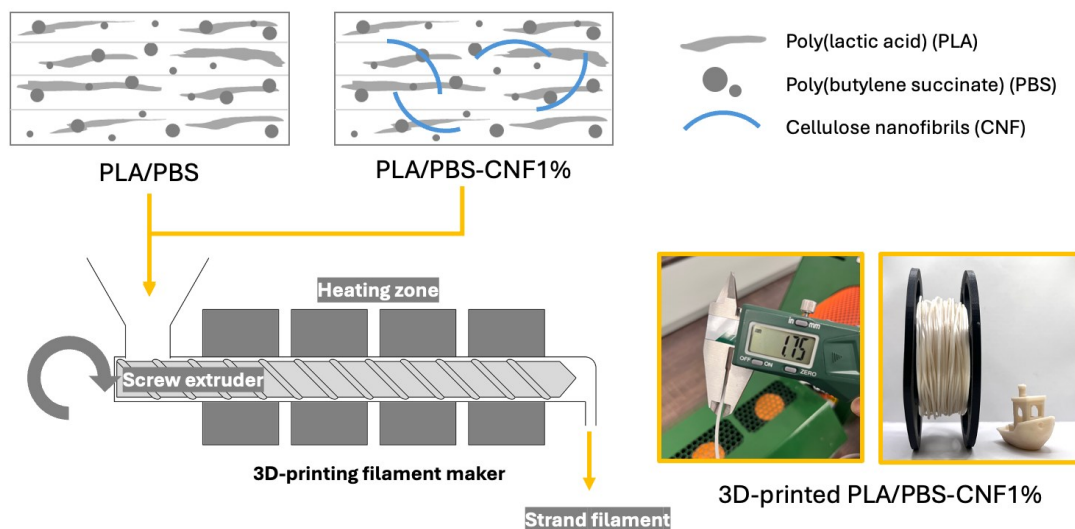
# Effect of Cellulose Nanofibrils in Direct Melt-Blending of Poly-(Lactic Acid) and Poly(Butylene Succinate) for 3D-Printing

Muhammad Alif Fitri Hanipa,<sup>a,b,c</sup> Siti Aisyah Syazwani Zaidi,<sup>a,b</sup> Wan Hafizi Wan Ishak,<sup>d</sup> and Mohd Shaiful Sajab <sup>a,b,\*</sup>


\* Corresponding author: mohdshaiful@ukm.edu.my

DOI: 10.15376/biores.21.1.1050-1064

## GRAPHICAL ABSTRACT



# Effect of Cellulose Nanofibrils in Direct Melt-Blending of Poly(Lactic Acid) and Poly(Butylene Succinate) for 3D-Printing

Muhammad Alif Fitri Hanipa,<sup>a,b,c</sup> Siti Aisyah Syazwani Zaidi,<sup>a,b</sup> Wan Hafizi Wan Ishak,<sup>d</sup> and Mohd Shaiful Sajib <sup>a,b,\*</sup>

Biopolymers, especially poly(lactic acid) (PLA), have been among major 3D-printing materials, particularly for fused deposition modelling (FDM) techniques. Blending of PLA with poly(butylene succinate) (PBS) can enhance toughness. The blend can be reinforced by the addition cellulose nanofibrils (CNF), which has been rarely studied. A 1% solution of CNF was added to PLA/PBS with ratio of 70:30 directly during melt-blending into 3D-printing filament, which was fed into a FDM 3D printer. Characterization by Fourier transform infrared spectroscopy revealed successful integration of CNF fillers with more hydroxyl group availability in the composite. The degree of crystallinity of PLA, however, was decreased by addition of CNF fillers. This was also evident by the X-ray diffraction analysis, probably due to reduced chain mobility by entanglement effect. Mechanical performance of the printed samples was studied at 23 °C and at slightly elevated temperature of 40 °C, which revealed improved modulus and elongation stability at 40 °C in PLA/PBS-CN1% composite. Water absorption study also revealed 50% enhancement with addition of CNF fillers, indicating improved water penetration, which could be beneficial for biodegradability. With good mechanical stability at around 40 °C and good water penetration, PLA/PBS-CN1% composite could be beneficial in 3D-printing for biomedical application and water treatment.

DOI: 10.15376/biores.21.1.1050-1064

**Keywords:** Polylactic acid; Polybutylene succinate; Cellulose nanofibrils; Bio-based composites

**Contact information:** *a: Research Center for Sustainable Process Technology (CESPRO), Faculty of Engineering and Built Environment, Universiti Kebangsaan Malaysia, 43600 Bangi, Selangor, Malaysia; b: Department of Chemical and Process Engineering, Faculty of Engineering and Built Environment, Universiti Kebangsaan Malaysia, 43600 Bangi, Selangor, Malaysia; c: Roobah Sdn. Bhd., Akademia Siber Teknopolis, Universiti Kebangsaan Malaysia, 43600 Bangi, Selangor, Malaysia; d: Department of Applied Physics, Faculty of Science and Technology, Universiti Kebangsaan Malaysia, 43600 Bangi, Selangor, Malaysia; \*Corresponding author: mohdshaiful@ukm.edu.my*

## INTRODUCTION

Additive manufacturing, especially in the 3D-printing area, has already gained special interests from scientific communities due to its immense potential in various application areas (Tappa *et al.* 2019; Tao *et al.* 2021; Gauss and Pickering 2023). Among the popular techniques being utilized is fused deposition modelling (FDM). This method is especially popular for polymers due to its flexibility with various types of polymeric materials and composites (Tao *et al.* 2021; Mukoroh *et al.* 2024). Poly-lactic acid (PLA) for examples has become integral part of FDM 3D-printing materials, especially being a

bio-based and biodegradable, which could be beneficial for sustainability and environmental preservation (Bhagia *et al.* 2021; Tao *et al.* 2021; Musa *et al.* 2022; Zaidi *et al.* 2023). It has considerable modulus due to being in glassy state as its glass transition temperature is generally above ambient temperature. However, the glassy state of PLA contributes to its low impact resistance and relative brittleness compared to several polymers such as polypropylene (PP) (Rosli *et al.* 2021; da Silva Barbosa Ferreira *et al.* 2022; Schmitz *et al.* 2023).

Blending of PLA with other ductile polymers such as poly-butylene succinate (PBS) has been shown to enhance ductility and toughness due to capability of PBS to achieve over 500% of elongation (Ostrowska *et al.* 2019; Su *et al.* 2019; Schmitz *et al.* 2023). Addition of PBS can add a plasticizing effect and improve energy-dissipating mechanisms contributing to high toughness, such as effective stress transfer along its backbone chain and multiple nanosized voids formation (Tangnorawich *et al.* 2023). Over 8-fold increase of elongation at break has been achieved by the FDM 3D-printed samples by blending with 50% w/w PBS compared to the neat PLA (Garofalo *et al.* 2025). Biodegradability of PBS is also advantageous for biodegradable polymer blends formulations with PLA, as PBS is also biodegradable (Garofalo *et al.* 2025). The interfacial region between PLA and PBS phases in PLA/PBS blends could enhance water penetration, thereby potentially further improving biodegradability (Lyyra *et al.* 2023). Although most of PBS production is still petroleum-based, fully bio-based PBS production has been growing, especially from the underutilized agricultural biomass (Qiu *et al.* 2016; Luthfi *et al.* 2020; Lyyra *et al.* 2023). A study on production of PBS from oil palm biomass has revealed high feasibility of producing 100% bio-based PBS with 99.69% purity, 6.33 years of dynamic payback period (Arpa *et al.* 2023). Fully bio-based especially from agricultural biomass leftovers could be highly valued due to rising concern on the environmental problems, especially related to the petroleum (Luthfi *et al.* 2020; Aliotta *et al.* 2022).

A high content of cellulosic materials in the agricultural biomass can be further utilized to reinforce PLA/PBS blends, which has been studied extensively with PLA and PBS (Cindradewi *et al.* 2021; Lafia-Araga *et al.* 2021; Shazleen *et al.* 2021; Ren *et al.* 2022; Hanipa *et al.* 2025). In both PLA and PBS-based cellulose composites, mechanical improvements have been reported (Cindradewi *et al.* 2021; Platnieks *et al.* 2021; Shazleen *et al.* 2021). PLA reinforced with cellulose nanofibrils (CNF) improved tensile strength and modulus by maximum of 8% and 14%, respectively, as reported by a previous study (Shazleen *et al.* 2021). Another study that formulated PBS with CNF has successfully improved tensile strength by up to 19%, however with the use of a coupling agent (Cindradewi *et al.* 2021). PLA/PBS blends composite with cellulosic materials have also been reported particularly with the use of agricultural fibers and crystalline cellulose such as microcrystalline cellulose (MCC) and cellulose nanocrystals (CNC) (Rasheed *et al.* 2021; Zhang *et al.* 2022; Garofalo *et al.* 2025; Ucpinar *et al.* 2025). For example, the effect of hemp fiber addition into PLA/PBS FDM 3D-printing filament has been investigated in a previous study, which observed improvement of flexural modulus but slight decrease of flexural strength (Garofalo *et al.* 2025). Another study reported over 22% of tensile strength improvement and over 1-fold of improvement of modulus with addition of 0.75% w/w CNC into PLA/PBS blends (Rasheed *et al.* 2021). One previous study has utilized CNF for PLA/PBS with notable improvement of hydrophilicity, protein adsorption, and cell proliferation rate, revealing its potential in biomedical studies (Saeed *et al.* 2022). The study however was focused on electrospinning, which is highly different than FDM 3D-printing. Despite having huge benefit and potentials, several challenges associated with

incorporation of fillers from biomass into FDM 3D-printing were reported, including nozzle clogging and flow inconsistency (Bhagia *et al.* 2021). Limited miscibility between PLA and PBS could also impose challenges, especially when adding cellulose fillers, albeit good compatibility of the fillers has been reported separately with PLA and PBS, respectively below 3% w/w of filler loading (Deng *et al.* 2015; Cindradewi *et al.* 2021; Shazleen *et al.* 2021).

The aim of this study was to investigate the effect of CNF addition to PLA/PBS formulation for 3D-printing applications. This involved the process of direct melt-compounding and extrusion into 3D-printing filaments by using a benchtop filament maker, which were fed into a 3D-printer to prepare samples for mechanical performance and water absorption study. The effect of CNF addition was observed in terms of chemical interactions, thermal stability properties, and crystallinity properties, in comparison to the PLA/PBS polymer blend.

## EXPERIMENTAL

### Materials

PLA pellets with brand name Luminy LX-575 were obtained from Total Corbion (Rayong, Thailand). The PLA pellets were reported to have a density, melt flow index, and stereoisomer purity, of 1.24 g/cm<sup>3</sup>, 7 g/10 min (210 °C/2.16 kg), and 98% L-isomer, respectively. Bio-based PBS pellets with a density, melting point, and melt flow index, of 1.21 g/cm<sup>3</sup>, 100 to 115 °C, and 2.5 to 4.5 g/10 min (190 °C/2.16 kg), respectively, were sourced from Xinjiang Blue Ridge Tunhe Polyesters Co., Ltd. (Xinjiang, China). CNF extracted from oil palm empty fruit bunch fibers (OPEFB) was sourced from Roobah Sdn. Bhd. (Selangor, Malaysia) following the previously reported method (Wan Jusoh *et al.* 2025).

Briefly, dissolved lignin was removed from OPEFB using an organosolv extraction process, where OPEFB fibers were mixed with 90% formic acid at a 30:1 ratio and heated in a three-neck flask at 90 °C for 2 h. The resulting pulp was separated by vacuum filtration and washed with deionized water. Catalytic oxidation was then performed using 30% hydrogen peroxide (1–6% w/v) and Fe(II) (2–14 mg/L) at 90 °C for 24 h, with ~0.1 mL of 1 M HCl added to stabilize the solution. All chemicals used in this process were obtained from Merck, Darmstadt, Germany. After filtration and washing, the purified cellulose pulp was stored at ~4 °C. To prepare cellulose nanofibrils (CNF), the isolated cellulose (0.7 wt%) was dispersed in deionized water and fibrillated for 30 min using a high-speed homogenizer (25,000 rpm, IKA T25 Digital, Staufen, IKA Germany), maintaining the temperature below 70 °C. The CNF suspension was stored at ~4 °C prior to drying. For CNF powder production, the suspension was subsequently spray-dried using an in-house laboratory spray-drying system to obtain dry CNF powder.

### Preparation of 3D-Printing Filament

CNF powder, PLA, and PBS pellets were heated at a temperature of 50 °C overnight to remove moisture before the extrusion to produce filaments to avoid hydrolytic degradation during the extrusion. The dried PLA and PBS pellets were weighed according to 70:30 ratio and mixed inside a beaker until obtaining well distributed PLA and PBS pellets. To produce a premix of PLA/PBS-CNF1%, 1% w/w of dry CNF powder was weighed. 1% v/w of chloroform was added into the beaker, and the CNF powder was

immediately added and mixed until the CNF homogeneously attached on the surface of the pellets by visual observation. The PLA/PBS-CNF1% premix then was kept in an oven at 50 °C for 30 min to allow complete drying before extrusion process.

For the PLA/PBS-CNF1% composite preparation, a benchtop filament maker (Filabot EX2 Extruder, Filabot, Barre, VT, USA) was used for this study. The extruder was pre-cleaned and purged with HDPE at 230 °C, followed by the desire polymer, PLA/PBS extrusion to purge the excess HDPE in accordance with the standard operating procedure of the extruder, as HDPE provides a low-viscosity and thermally stable melt that effectively removes residual materials. The premix of PLA/PBS of was fed into the filament maker at a minimum of 100 g until PLA/PBS started to be extruded, after which the temperature of 165 and 175 °C at feeding and at the nozzle, respectively were used. The filament diameter was continuously measured and controlled by the diameter control package of the filament maker to ensure consistent diameter of  $1.75 \pm 0.10$  mm. After PLA/PBS finished, premix of PLA/PBS-CNF1% was fed and the same extrusion process was carried out to produce PLA/PBS-CNF1% filament.

### 3D-Printing Process

Samples for tensile and impact testing were prepared through fused deposition modelling (FDM) 3D-printing technique using Prusa i3 MK3S (Prusa Research, Prague, Czech Republic). The tensile sample design was based on ASTM D638 Type V, while the water absorption test was based on ASTM D570 (76.2 mm × 25.4 mm × 3.2 mm). All designs were converted to G-code by using PrusaSlicer software 2.7.4 (Prusa Research, Prague, Czech Republic) by using vertical shell consisting of 2 perimeter lines, and a rectilinear infill of 100% at an angle of 45°. Nozzle temperatures of 215 and 205 °C were used for the first layer and the remaining layers, respectively, while a constant printer bed temperature of 60 °C was used.

### Water Absorption Study

3D-printed ASTM D570 samples were dried overnight using an oven at temperature 50 °C. The samples were taken out and left cooled in a desiccator for 2 h before being weighed using a high precision balance to get the initial weight,  $w_0$ . The samples then were fully immersed in deionized water and kept at 23 °C. The wet weight of each sample at each determined time,  $w_t$  was measured by wiping the surface of sample with lint free dry tissue before being weighed using the precision balance. Water absorption at a specific time was calculated using the following Eq. 1 (Lagazzo *et al.* 2025).

$$\text{Water Absorption} = \left[ \frac{w_t - w_0}{w_0} \right] \times 100 \quad (1)$$

### Characterization

Fourier transform infrared spectrophotometric analysis was carried out to study chemical bonding in both PLA/PBS and PLA/PBS-CNF1% using an IRSpirit attenuated total reflectance FTIR spectrophotometer (ATR-FTIR; Shimadzu, Kyoto, Japan). A resolution of 1.0 cm<sup>-1</sup> was used for this study covering from 4000 to 400 cm<sup>-1</sup> of spectral range.

Thermogravimetric analysis (TGA) was carried out at a rate of 20 °C/min from room temperature of 25 to 600 °C, to study thermal degradation of the filaments. Thermal properties of both compositions were also assessed by differential scanning calorimetry



(DSC). This involved a heating the sample at a rate of 10 °C/min from 25 to 200 °C for the initial heating phase, followed by cooling from 200 to -60 °C, and a second heating from minus 60 °C to 200 °C. The degree of crystallinity of was determined using the melting enthalpy ( $\Delta H_m$ ) and cold crystallization ( $\Delta H_{cc}$ ) obtained from the DSC, using Eq. 2, where  $\Delta H_m^*$  is the heat of fusion of PLA (93 J/g) and  $w$  represents the weight fraction of PLA (He *et al.* 2023; Ucpinar *et al.* 2025).

$$X_c = \left[ \frac{\Delta H_m - \Delta H_{cc}}{\Delta H_m^* \times w} \right] \times 100 \quad (2)$$

X-ray diffraction (XRD) was used to study the crystal structures in the samples using a D8 Advance (Bruker AXS, Germany) XRD machine  $2\theta$  range of 3° to 50°, with  $\text{CuK}\alpha$ -1 as radiation source ( $\lambda = 0.15406$  nm). The crystallinity index (CrI), was calculated based on the integrated intensity of peak signals due to crystalline phase ( $I_{crystal}$ ) and amorphous phase ( $I_{amorphous}$ ), based on following equation (Eq. 3).

$$CrI = \left[ \frac{I_{crystal}}{I_{crystal} + I_{amorphous}} \right] \times 100 \quad (3)$$

Mechanical performance was evaluated through tensile testing of 3D-printed sample prepared according to ASTM D638 standards. Tests were conducted using an Instron® Electromechanical Universal Testing System (3300 Series) equipped with a 1 kN load cell, at a crosshead speed of 10 mm/min. Morphology and microstructural viewing of the filament cross-section and fracture sites of 3D-printed tensile samples, were observed using a field emission scanning electron microscopy (FESEM) (Merlin Compact, Zeiss Pvt. Ltd., Oberkochen, Germany).

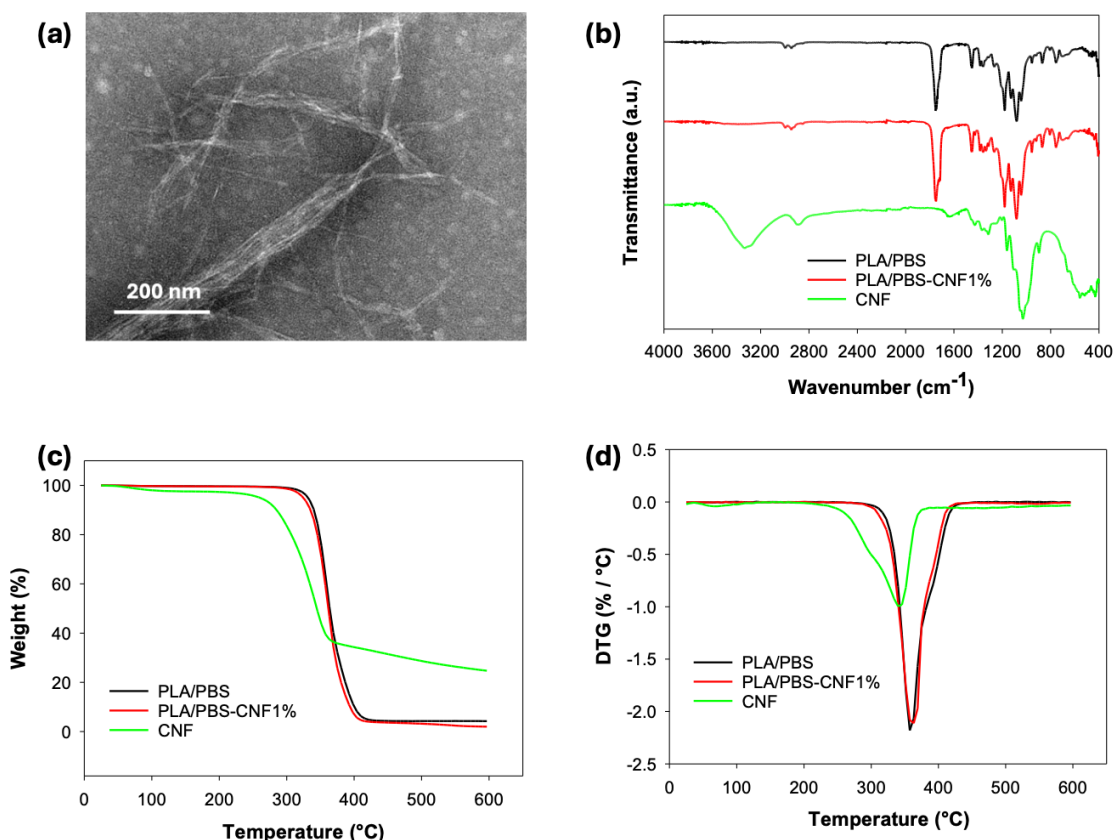
## RESULTS AND DISCUSSION

### Structural and Thermal Characterization of PLA/PBS-CNF

The prepared CNF was characterized to examine its morphological properties. As shown in Fig. 1(a), the CNF exhibited a well-dispersed fibrillar network. TEM analysis confirmed fibril diameters in the range of 10 to 30 nm, indicating effective size reduction during mechanical fibrillation. These dimensions are consistent with the authors' previous findings, further validating the efficiency of the CNF isolation and disintegration process (Wan Jusoh *et al.* 2025). Fourier transform infrared spectroscopy (FTIR) was carried out on PLA/PBS-CNF1% filament to study the interaction between the chemical structures of PLA, PBS, and CNF. Based on the FTIR absorption spectra in Fig. 1a, a strong and wide absorbance peak can be seen at 3000 to 3600  $\text{cm}^{-1}$ , representing bending of hydroxyl (O-H) group in CNF, similar to a previous study (Jakka *et al.* 2025). A similar wide absorbance peak at 3000 to 3600  $\text{cm}^{-1}$  due to O-H bending in the CNF, was observed in PLA/PBS-CNF1% because of the presence of more hydroxyl groups contributed by the 1% CNF fillers. A slight increase in the absorbance at 1336  $\text{cm}^{-1}$  and a shoulder at 1163  $\text{cm}^{-1}$  can be attributed to O-H bending and C-O stretching vibration, respectively, in CNF fillers. Such features were shown in absorbance spectra of PLA/PBS-CNF1% as in Fig. 1b (Jakka *et al.* 2025).

Thermal degradation properties were analysed by TGA, as shown in Fig. 1b. It is apparent that the weight loss of CNF started at around 250 °C, probably contributed by the

degradation of cellulose chain (Hanipa *et al.* 2025). The CNF reached maximum degradation at around 340 °C. Beyond 375 °C, the weight loss still could be observed at a significantly lower rate, probably attributed to the oxidation and degradation of short-chain cellulose into lower molecular weight and volatile products (Hanipa *et al.* 2025). The weight of PLA/PBS and PLA/PBS-CNF1% started to drop at 320 and 310 °C, respectively, as shown in Fig. 1c. The DTG curves in Fig. 1d shows that the degradation rate of the composite filament PLA/PBS-CNF1% was only slightly lower than PLA/PBS control sample, indicating minimal improvement of thermal degradation stability by CNF addition.

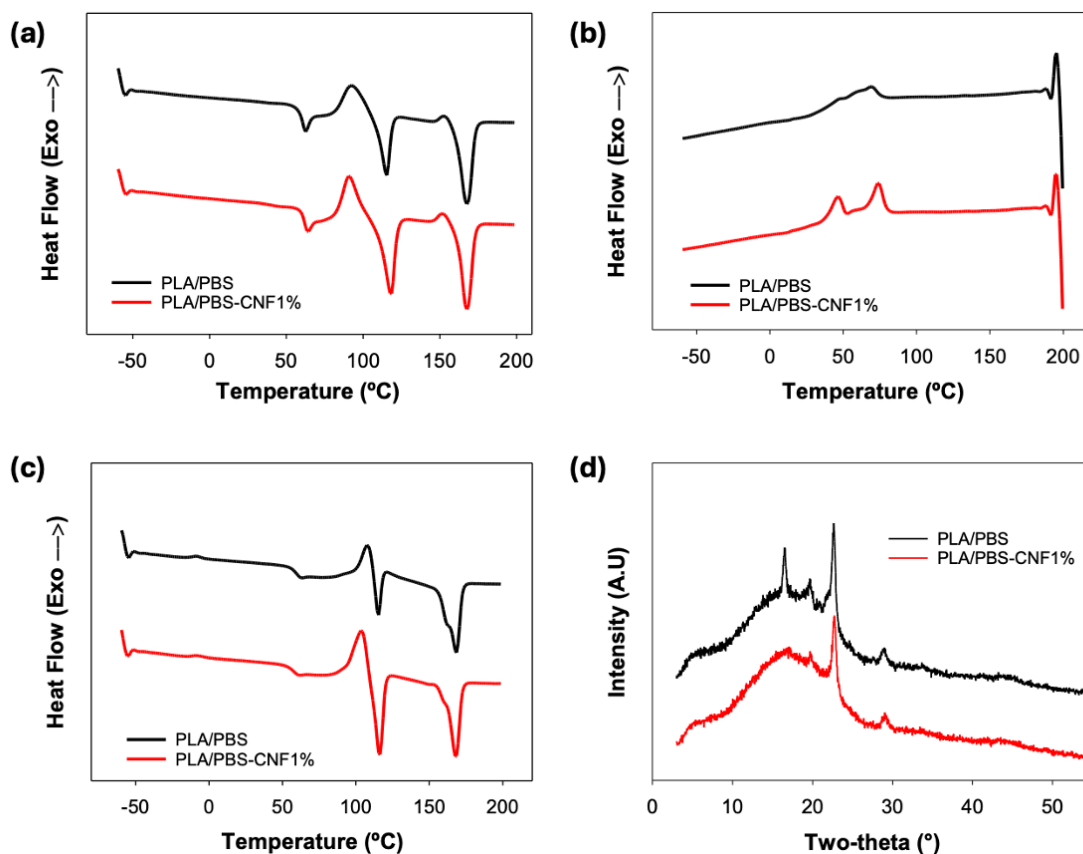


**Fig. 1.** (a) TEM micrograph of CNF and (b) FTIR absorption spectra, (c) TGA analysis, (d) DTG (c), for CNF, PLA/PBS, PLA/PBS-CNF1%.

Differential scanning calorimetry (DSC) was carried out to examine the thermal properties of PLA/PBS and PLA/PBS-CNF1% in the range of -50 to 200 °C. A narrower peak of cold crystallization can be observed in PLA/PBS-CNF-1% in Fig. 2a. The  $T_{cc}$  was also lower in PLA/PBS-CNF1%, as shown by Table 1, indicating potential CNF nucleation effect similar to other studies (Shazleen *et al.* 2021). In the cooling scan, higher  $T_c$  of PBS phase at 73.8 °C was observed in PLA/PBS-CNF1%, indicating nucleation effect of CNF fillers on the PBS phase (Cindradewi *et al.* 2021). A clear second exothermic peaks were observed in PLA/PBS-CNF1% at 46.3 °C, compared to PLA/PBS, probably hinting trans-crystallization of PBS during the cooling scan (Platnieks *et al.* 2020). A second heating scan showed lower cold crystallization peak in PLA/PBS as the slower DSC cooling scan compared to during extrusion, allowing for better rearrangement of PLA/PBS. In PLA/PBS-CNF1%, chain entanglement effect by CNF fillers could restrict chain mobility

during the DSC cooling scan, therefore there was only a small decrease of  $T_{cc}$  in the second heating (Wang *et al.* 2020; Cindradewi *et al.* 2021).

The movement restriction could also be the reason for the drop of XRD intensity as shown by Fig. 2d, especially at  $16.5^\circ$  representing (110/200) crystal plane of PLA. PLA/PBS blends have been known to increase crystallinity of PLA phase compared to the neat PLA, due to the heterogeneous nucleation effect by the PBS phase (Deng and Thomas 2015; Su *et al.* 2019). Addition of the CNF fillers could interrupt the crystallization process due to the entanglement effect, which reduces chain mobility (Wang *et al.* 2020; Cindradewi *et al.* 2021). A slight intensity drop was also shown by Fig. 2d at  $19.6^\circ$  and  $22.6^\circ$ , which represent (020) and (110) crystal planes of PBS, respectively. A previous study also reported decrease in the degree of crystallinity of PBS with addition of CNF (Cindradewi *et al.* 2021). The degree of crystallinity of PLA, which was calculated based on DSC thermal properties, also showed a drop in the PLA/PBS-CNF1%, as reported in Table 1. Similarly, the crystallinity index of PLA/PBS also showed a decrease as shown by Table 1.



**Fig. 2.** (a) DSC first heating scan, (b) cooling scan, (c) second heating scan, and (d) XRD diffractogram for PLA/PBS and PBS/PBS-CNF1%

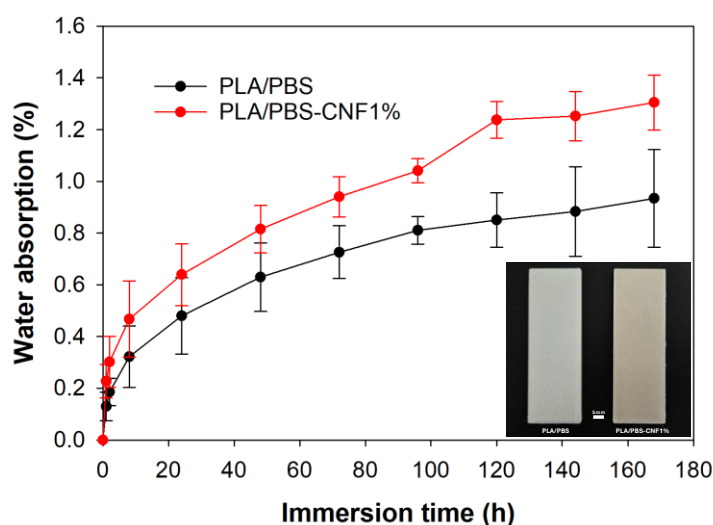
**Table 1.** Thermal and Crystallinity Properties PLA/PBS and PLA/PBS-CNF1%

Filament	$T_g$ , PLA (°C)	$T_c$ , PBS (°C)	$T_{cc}$ , PLA (°C)	$T_m$ , PLA (°C)	$\Delta H_{cc}$ (J/g)	$\Delta H_m$ , PLA (J/g)	$X_{c,PLA}$ (%)	CrI (%)
PLA/PBS	59.3	68.8	92.0	167.6	15.7	28.7	19.8	12.9
PLA/PBS-CNF1%	56.6	73.8	90.8	167.6	19.5	24.0	6.9	9.3



### Physical and Mechanical Characterization of 3D-printed PLA/PBS-CNF

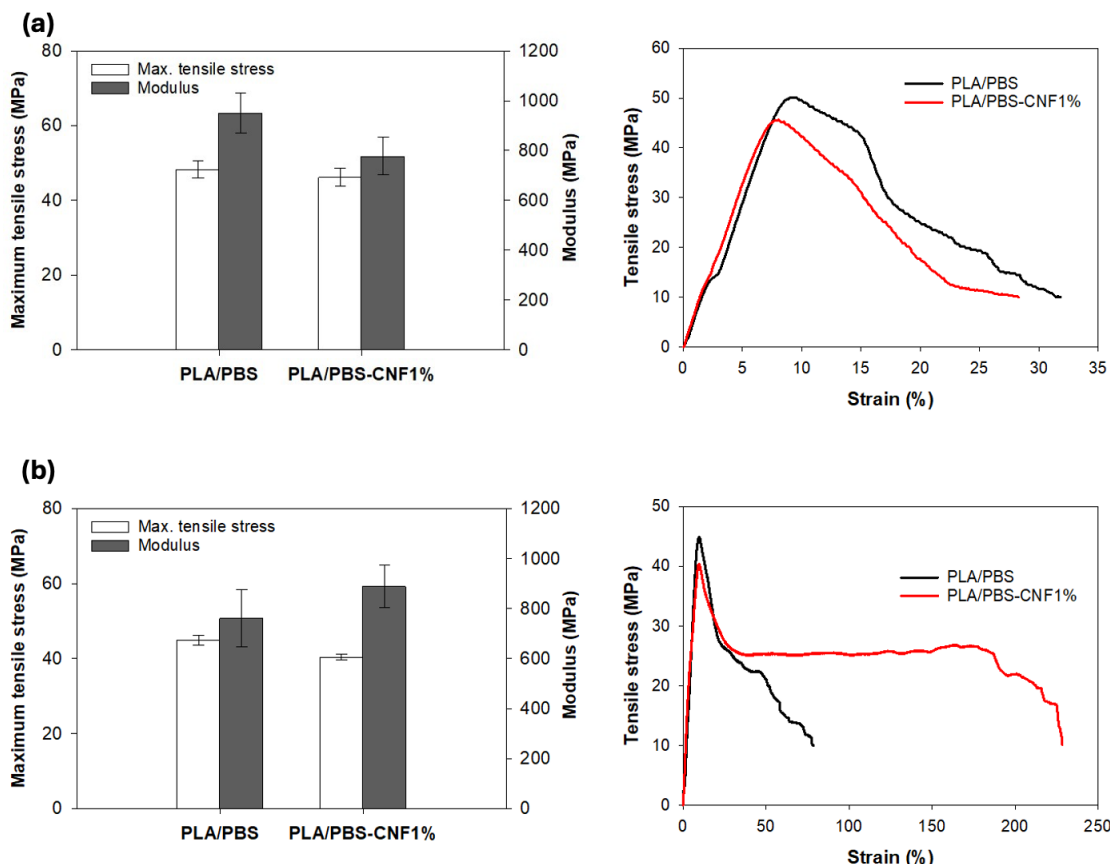
Water absorption tests according to ASTM D570 were carried out, using 3D-printed samples of PLA/PBS-CNF1%, with PLA/PBS sample as control, as depicted in Fig. 3. Addition of CNF has been shown to alter the color of the 3D-printed samples towards slightly brown due to the effect of high heat on the CNF, as shown in the authors' previous study of PLA-CNF composites (Hanipa *et al.* 2025). The water absorption profiles in Fig. 3 reveal that addition of 1% CNF increased the water absorption ability by 50%, thanks to the excellent hydrophilicity of CNF. A similar study focusing on CNF nanocomposite based on PLA plasticized by PEG also reported similar water absorption increases by CNF addition (Wolf *et al.* 2023). Significant increasing of water absorption could indicate promotion of water penetration in PLA/PBS-CNF1% composite FDM 3D-printed samples, which could help to further improve biodegradability of the materials (Rosli *et al.* 2021; Lyyra *et al.* 2023).



**Fig. 3.** Water absorption study for the 3D-printed PLA/PBS and PLA/PBS-CNF1%

In terms of mechanical properties of the printed samples, the addition of CNF slightly decreased the maximum tensile strength and modulus at 23 °C, as shown by Fig. 4a. The decrease was possibly due to agglomeration of CNF fillers and microphase separation, preventing effective transfer of stress throughout the matrix, especially at room temperature of 23 °C (Rasheed *et al.* 2021). Similar profiles of the stress-strain curves for both PLA/PBS and PLA/PBS-CNF1% were observed at testing temperature 23 °C, as depicted in Fig. 4a, probably due to less freedom for the chain movement at 23 °C, especially for FDM 3D-printed samples.

At slightly elevated temperature of 40 °C, both PLA/PBS and PLA/PBS-CNF1% exhibited lower maximum tensile stress and longer tensile strain than at room temperature, as shown by Fig. 4(b). At 40 °C, PLA/PBS polymer chains have more freedom to undergo plastic deformation than at 23 °C, contributing to longer strain (Dmitruk *et al.* 2023). While PLA/PBS-CNF1% achieved slightly lower maximum tensile strength, the modulus and the elongation at break were higher than in PLA/PBS, as shown by Table 2. Reinforcement effect by the CNF in PLA matrix might be the reason for the increased modulus at 40 °C, similar to previous studies (Garofalo *et al.* 2025; Hanipa *et al.* 2025).



**Fig. 4.** Tensile properties (left) and stress-strain curves (right) for testing temperature of (a) 23 °C and (b) 40 °C

The stress-strain curves at 40 °C in Fig. 4(b) reveal better stability of the PLA/PBS-CNF1% composite up to around 170% strain, maintaining tensile strength at above 25 MPa, compared to the PLA/PBS. Better stability at slightly elevated temperature of 40 °C could be promoted by the chain entanglement by CNF addition, allowing for effective elongation of PBS phase (Platnieks *et al.* 2021). The stability of PBS elongation by CNF contributes to the overall higher elongation by PLA/PBS-CNF1% at 40 °C, as shown by Table 2. Enhanced modulus and elongation of PLA/PBS-CNF1% at 16.8% and 62.7% were higher than PLA/PBS, respectively. The slight decrease of tensile strength of 10.0% could be beneficial for biomedical-related applications that need stiffness and resistance to brittle fracture while operating near body temperature of around 37 °C, such as in orthopaedics.

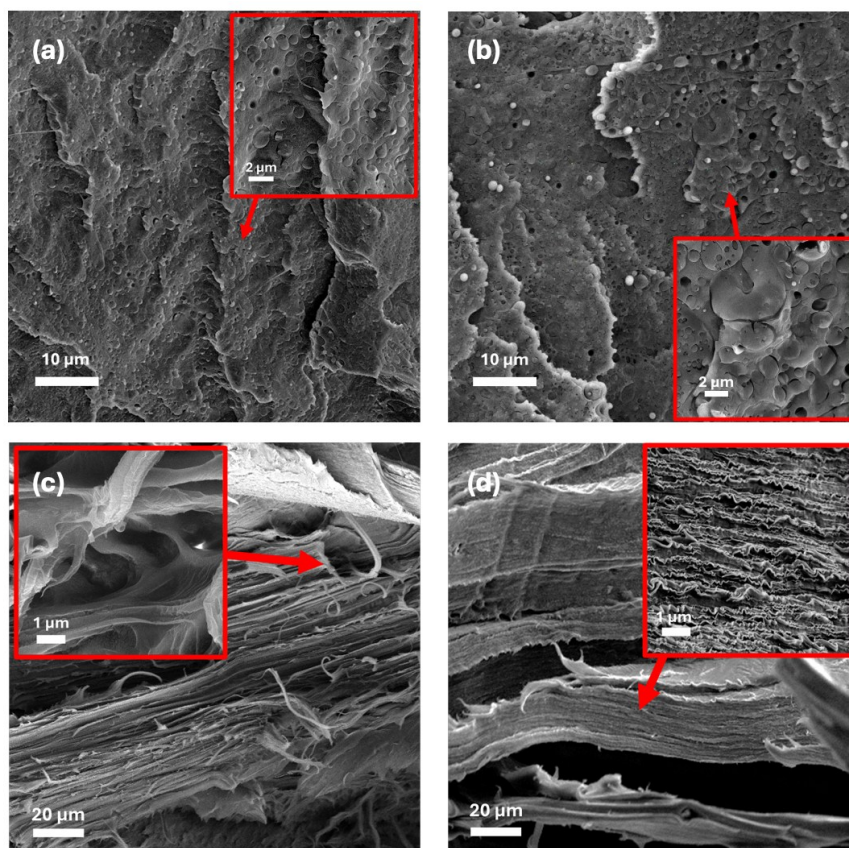
**Table 2.** Tensile Properties of the Printed PLA/PBS and PLA/PBS-CNF1% at Testing Temperatures of 23 °C and 40 °C, Respectively

Sample	Testing T (°C)	Max. Tensile Stress (MPa)	Modulus (MPa)	Strain at Break (%)
PLA/PBS	23	48.3 ± 2.2	949.9 ± 79.9	33.2 ± 7.0
PLA/PBS-CNF1%	23	46.2 ± 2.3	777.8 ± 76.2	28.6 ± 7.4
PLA/PBS	40	44.9 ± 1.3	761.2 ± 113.8	110.5 ± 46.7
PLA/PBS-CNF1%	40	40.4 ± 0.7	889.1 ± 83.6	179.8 ± 88.9

### Micrograph of PLA/PBS-CNF

The morphologies of the cross-section of filaments of PLA/PBS filament and PLA/PBS-CNF1% composite filament are shown in Fig. 5. A higher concentration of voids can be seen in the cross-section of PLA/PBS-CNF1% composite filament than in PLA/PBS in Figs. 5a-b. Under higher magnification of the area marked by the red arrow, higher variation of the PBS droplets size can also be observed for the PLA/PBS-CNF1% composite in Fig. 5b. A larger PBS phase can also be seen in the PLA/PBS-CNF1% composite, which could indicate possibility of having co-continuous phase of PBS as reported in a previous study (Deng and Thomas 2015).

CNF fillers could induce a heterogeneous nucleation effect on both molten PLA and PBS, causing even faster nucleation hence larger variations of PBS phase in PLA matrix (Shazleen *et al.* 2021). Restriction of chain movement of both PLA and PBS caused by chain entanglement with CNF fillers could also influence the variation of PBS phase in PLA matrix (Platnieks *et al.* 2021; Hanipa *et al.* 2025). Tensile fracture morphology revealed fibre pull-out in both PLA/PBS and PLA/PBS-CNF1% due to elongated PBS droplets during tensile testing in Figs. 5c-d. Fine elongated PBS fibre pull-out with thickness of below 1.0  $\mu\text{m}$  can be observed in the PLA/PBS-CNF1%, as shown in Fig. 5d. The fine elongated fibres were mostly still attached to the neighbouring elongated fibres, indicating improved stability of the elongated fibre by chain entanglement with addition of 1% w/w of CNF fillers (Platnieks *et al.* 2020).



**Fig. 5.** Morphology of 3D-printed filament cross-section of (a) PLA/PBS, (b) PLA/PBS-CNF1%, and tensile fractures of (c) PLA/PBS and (d) PLA/PBS-CNF1%

## CONCLUSIONS

1. In conclusion, 1% w/w of CNF was successfully added into PLA/PBS through direct melt-blending into 3D-printing filaments and was 3D-printed. The CNF addition slightly decreased mechanical strength of PLA/PBS at room temperature, which was attributable to the decrease of crystallinity and potential agglomeration of CNF fillers.
2. Improved elongation stability at slightly elevated temperature of 40 °C was observed in PLA/PBS-CNF1% composite, probably due to effective entanglement between elongated PBS molecular chains.
3. Thermal degradation stability was slightly reduced by the addition of CNF. However significant improvement of water absorption capability was achieved by 50% increase with CNF addition, which could be beneficial for biomedical and water treatment application.

## ACKNOWLEDGMENTS

We gratefully acknowledge the financial and technical support provided by the Ministry of Science, Technology and Innovation (MOSTI), Malaysia through the grant provided under Technology Development Fund 2 (TeD 2) [grant number TEF08241295] and Universiti Kebangsaan Malaysia-Yayasan Sime Darby (UKM-YSD) Chair for Sustainability. During the preparation of this work, the authors used ChatGPT to improve language and readability. After using this tool, the authors have reviewed and edited the content as needed and take full responsibility for the content of the publication.

## REFERENCES CITED

- Aliotta, L., Seggiani, M., Lazzeri, A., Gigante, V., and Cinelli, P. (2022), “A brief review of poly(butylene succinate)(PBS) and its main copolymers: synthesis, blends, composites, biodegradability, and applications,” *Polymers* 14(4), article 844.  
<https://doi.org/10.3390/polym14040844>
- Arpa, R., Luthfi, A. A. I., Bukhari, N. A., Tan, J. P., Mahmud, S. S., and Salleh, M. Z. M. (2023). “Economical study of bio-based polybutylene succinate production from oil palm biomass,” *J. Oil Palm Res.* 35(4), 682-693.  
<https://doi.org/10.21894/jopr.2023.0001>
- ASTM D638-14 (2014). “Standard test method for tensile properties of plastics,” ASTM International, West Conshohocken, PA. <https://doi.org/10.1520/D3345-08>
- ASTM D570-98 (2018). “Standard test method for water absorption of plastics,” ASTM International, West Conshohocken, PA. <https://doi.org/10.1520/D3345-08>
- Bhagia, S., Bornani, K., Agrawal, R., Satlewal, A., Đurković, J., Lagaña, R., Bhagia, M., Yoo, C. G., Zhao, X., Kunc, V., Pu, Y., Ozcan, S., and Ragauskas, A. J. (2021). “Critical review of FDM 3D printing of PLA biocomposites filled with biomass resources, characterization, biodegradability, upcycling and opportunities for biorefineries,” *App. Mater. Today* 24, article 101078.  
<https://doi.org/10.1016/j.apmt.2021.101078>



- Cindradewi, A. W., Bandi, R., Park, C. W., Park, J. S., Lee, E. A., Kim, J. K., Kwon, G.-J., Han, S.-Y., and Lee, S. H. (2021). "Preparation and characterization of polybutylene succinate reinforced with pure cellulose nanofibril and lignocellulose nanofibril using two-step process," *Polymers* 13(22), article 3945. <https://doi.org/10.3390/polym13223945>
- da Silva Barbosa Ferreira, E., Luna, C. B. B., Siqueira, D. D., Araújo, E. M., de França, D. C., and Wellen, R. M. R. (2022). "Annealing effect on pla/eva blends performance," *Journal of Polymers and the Environment* 30(2), 541-554. <https://doi.org/10.1007/s10924-021-02220-4>
- Deng, Y., and Thomas, N. L. (2015). "Blending poly (butylene succinate) with poly (lactic acid): Ductility and phase inversion effects," *European Polymer Journal* 71, 534-546. <https://doi.org/10.1016/j.eurpolymj.2015.08.029>
- Dmitruk, A., Ludwiczak, J., Skwarski, M., Makuła, P., and Kaczyński, P. (2023). "Influence of PBS, PBAT and TPS content on tensile and processing properties of PLA-based polymeric blends at different temperatures," *Journal of Materials Science* 58(4), 1991-2004. <https://doi.org/10.1007/s10853-022-08081-z>
- Garofalo, E., Di Maio, L., and Incarnato, L. (2025). "PLA/PBS biocomposites for 3D FDM manufacturing: Effect of hemp shive content and process parameters on printing quality and performances," *Polymers* 17(17), article 2280. <https://doi.org/10.3390/polym17172280>
- Gauss, C., and Pickering, K. L. (2023). "A new method for producing polylactic acid biocomposites for 3D printing with improved tensile and thermo-mechanical performance using grafted nanofibrillated cellulose," *Additive Manufacturing* 61, article 103346. <https://doi.org/10.1016/j.addma.2022.103346>
- Hanipa, M. A. F., Zaidi, S. A. S., Sajab, M. S., Abdul, P. M., and Jamil, K. (2025). "Comparative study of blending techniques in polylactic acid/cellulose nanofibrils green composites for benchtop 3D printing filaments," *Polymer Composites* 46(4), 3070-3083. <https://doi.org/10.1002/pc.29154C>
- He, X., Tang, L., Zheng, J., Jin, Y., Chang, R., Yu, X., Song, Y., and Huang, R. (2023). "A novel UV barrier poly (lactic acid)/poly (butylene succinate) composite biodegradable film enhanced by cellulose extracted from coconut shell," *Polymers* 15(14), article 3000. <https://doi.org/10.3390/polym15143000>
- Jakka, V., Goswami, A., Nallajarla, A. K., Roy, U., Srikanth, K., and Sengupta, S., (2023). "Coconut coir-derived nanocellulose as an efficient adsorbent for removal of cationic dye safranin-O: A detailed mechanistic adsorption study," *Environmental Science and Pollution Research* 32, 19026–19047. <https://doi.org/10.1007/s11356-023-29075-7>
- Lafia-Araga, R. A., Sabo, R., Nabinejad, O., Matuana, L., and Stark, N. (2021). "Influence of lactic acid surface modification of cellulose nanofibrils on the properties of cellulose nanofibril films and cellulose nanofibril–poly (Lactic acid) composites," *Biomolecules* 11(9), article 1346. <https://doi.org/10.3390/biom11091346>
- Lagazzo, A., Moliner, C., Finocchio, E., Caputo, S., and Arato, E. (2025). "Hydrolytic degradation and assessment of performance of PLA and PBS-based plastics designed for packaging applications," *International Journal of Polymer Science* 2025(1), article 5602847. <https://doi.org/10.1155/ijps/5602847>



- Luthfi, A. A. I., Tan, J. P., Isa, N. F. A. M., Bukhari, N. A., Shah, S. S. M., Mahmud, S. S., and Jahim, J. M. (2020). "Multiple crystallization as a potential strategy for efficient recovery of succinic acid following fermentation with immobilized cells," *Bioprocess and Biosystems Engineering* 43(7), 1153-1169. <https://doi.org/10.1007/s00449-020-02311-x>
- Lyyra, I., Sandberg, N., Parihar, V. S., Hannula, M., Huhtala, H., Hyttinen, J., Massera, J., and Kellomäki, M. (2023). "Hydrolytic degradation of polylactide/polybutylene succinate blends with bioactive glass," *Materials Today Communications* 37, article 107242. <https://doi.org/10.1016/j.mtcomm.2023.107242>
- Mukoroh, P. F., Gouda, F., Skrifvars, M., and Ramamoorthy, S. K. (2024). "Influence of the manufacturing method (3D printing and injection molding) on water absorption and mechanical and thermal properties of polymer composites based on poly(lactic acid)," *Polymers* 16(12), article 1619. <https://doi.org/10.3390/polym16121619>
- Musa, L., Kumar, N. K., Abd Rahim, S. Z., Rasidi, M. S. M., Rennie, A. E. W., Rahman, R., Yousefi Kanani, A., and Azmi, A. A. (2022). "A review on the potential of polylactic acid based thermoplastic elastomer as filament material for fused deposition modelling," *Journal of Materials Research and Technology* 20, 2841-2858. <https://doi.org/10.1016/j.jmrt.2022.08.057>
- Ostrowska, J., Sadurski, W., Paluch, M., Tyński, P., and Bogusz, J. (2019). "The effect of poly (butylene succinate) content on the structure and thermal and mechanical properties of its blends with polylactide," *Polymer International* 68(7), 1271-1279. <https://doi.org/10.1002/pi.5814>
- Platnieks, O., Gaidukovs, S., Barkane, A., Sereda, A., Gaidukova, G., Grase, L., Thakur, V. K., Filipova, I., Fridrihsone, V., Skute, M., and Laka, M. (2020). "Bio-based poly (butylene succinate)/microcrystalline cellulose/nanofibrillated cellulose-based sustainable polymer composites: Thermo-mechanical and biodegradation studies," *Polymers* 12(7), article 1472. <https://doi.org/10.3390/polym12071472>
- Platnieks, O., Sereda, A., Gaidukovs, S., Thakur, V. K., Barkane, A., Gaidukova, G., Filipova, I., Ogurcovs, A., and Fridrihsone, V. (2021). "Adding value to poly (butylene succinate) and nanofibrillated cellulose-based sustainable nanocomposites by applying masterbatch process," *Industrial Crops and Products* 169, article 113669. <https://doi.org/10.1016/j.indcrop.2021.113669>
- Qiu, T. Y., Song, M., and Zhao, L. G. (2016). "Testing, characterization and modelling of mechanical behaviour of poly (lactic-acid) and poly (butylene succinate) blends," *Mechanics of Advanced Materials and Modern Processes* 2(1), article 7. <https://doi.org/10.1186/s40759-016-0014-9>
- Rasheed, M., Jawaid, M., and Parveez, B. (2021). "Bamboo fiber based cellulose nanocrystals/poly (Lactic acid)/poly (butylene succinate) nanocomposites: Morphological, mechanical and thermal properties," *Polymers* 13(7), article 1076. <https://doi.org/10.3390/polym13071076>
- Ren, Q., Wu, M., Wang, L., Zheng, W., Hikima, Y., Semba, T., and Ohshima, M. (2022). "Light and strong poly (lactic acid)/cellulose nanofiber nanocomposite foams with enhanced rheological and crystallization property," *The Journal of Supercritical Fluids* 190, article 105758. <https://doi.org/10.1016/j.supflu.2022.105758>
- Rosli, N. A., Karamanlioglu, M., Kargarzadeh, H., and Ahmad, I. (2021). "Comprehensive exploration of natural degradation of poly (lactic acid) blends in various degradation media: A review," *International Journal of Biological Macromolecules* 187, 732-741. <https://doi.org/10.1016/j.ijbiomac.2021.07.196>

- Saeed, U., Abdullah, T., and Al-Turaif, H. (2022). "Surface morphology and biochemical characteristics of electrospun cellulose nanofibril reinforced PLA/PBS hollow scaffold for tissue engineering," *Fibers and Polymers* 23(9), 2539-2548. <https://doi.org/10.1007/s12221-022-4229-6>
- Schmitz, L., Harada, J., Ribeiro, W. B., Rosa, D. S., and Brandalise, R. N. (2023). "Toughening of poly (lactic acid)(PLA) with poly (butylene adipate-co-terephthalate)(PBAT): A morphological, thermal, mechanical, and degradation evaluation in a simulated marine environment," *Colloid and Polymer Science* 301(12), 1405-1419. <https://doi.org/10.1007/s00396-023-05157-3>
- Shazleen, S. S., Yasim-Anuar, T. A. T., Ibrahim, N. A., Hassan, M. A., and Ariffin, H. (2021). "Functionality of cellulose nanofiber as bio-based nucleating agent and nano-reinforcement material to enhance crystallization and mechanical properties of polylactic acid nanocomposite," *Polymers* 13(3), article 389. <https://doi.org/10.3390/polym13030389>
- Su, S., Kopitzky, R., Tolga, S., and Kabasci, S. (2019). "Polylactide (PLA) and its blends with poly (butylene succinate)(PBS): A brief review," *Polymers* 11(7), article 1193. <https://doi.org/10.3390/polym11071193>
- Tangnorawich, B., Magmee, A., Roungpaisan, N., Toommee, S., Parcharoen, Y., and Pechyen, C. (2023). "Effect of polybutylene succinate additive in polylactic acid blend fibers via a melt-blown process," *Molecules* 28(20), article 7215. <https://doi.org/10.3390/molecules28207215>
- Tao, Y., Kong, F., Li, Z., Zhang, J., Zhao, X., Yin, Q., Xing, D., and Li, P. (2021). "A review on voids of 3D printed parts by fused filament fabrication," *Journal of Materials Research and Technology* 15, 4860-4879. <https://doi.org/10.1016/j.jmrt.2021.10.108>
- Tappa, K., Jammalamadaka, U., Weisman, J. A., Ballard, D. H., Wolford, D. D., Pascual-Garrido, C., Wolford, L. M., Woodard, P. K., and Mills, D. K. (2019). "3D printing custom bioactive and absorbable surgical screws, pins, and bone plates for localized drug delivery," *Journal of Functional Biomaterials* 10(2), article 17. <https://doi.org/10.3390/jfb10020017>
- Ucpinar, B., Sivrikaya, T., and Aytac, A. (2025). "Sustainable hemp fiber reinforced polylactic acid/poly (butylene succinate) biocomposites: Assessing the effectiveness of MAH-g-PLA as a compatibilizer," *Polymer Composites* 46(10), 9438-9453. <https://doi.org/10.1002/pc.29569>
- Wan Jusoh, W. N. L., Sajab, M. S., Mohd Yasin, N. H., Abdul, P. M., and Takriff, M. S. (2025). "Interaction of *Chlorella vulgaris*: Cell Attachment on nanocellulose-based hydrogel for sustainable microalgae cultivation," *BioResources* 20(1), 201-208. <https://doi.org/10.15376/biores.20.1.201-218>
- Wang, Q., Ji, C., Sun, J., Zhu, Q., and Liu, J. (2020). "Structure and properties of polylactic acid biocomposite films reinforced with cellulose nanofibrils," *Molecules* 25(14), article 3306. <https://doi.org/10.3390/molecules25143306>
- Wolf, M. H., Gil-Castell, O., Cea, J., Carrasco, J. C., and Ribes-Greus, A. (2023). "Degradation of plasticised poly (lactide) composites with nanofibrillated cellulose in different hydrothermal environments," *Journal of Polymers and the Environment* 31(5), 2055-2072. <https://doi.org/10.1007/s10924-022-02711-y>
- Zaidi, S. A. S., Kwan, C. E., Mohan, D., Harun, S., Luthfi, A. A. I., and Sajab, M. S. (2023). "Evaluating the stability of PLA-lignin filament produced by bench-top

extruder for sustainable 3D printing,” *Materials* 16(5), article 1793.

<https://doi.org/10.3390/ma16051793>

Zhang, X., Shi, J., Zhou, J., and Nan, J. (2022). “Nucleation effect of cellulose nanocrystals/polybutylene succinate composite filler on polylactic acid/polybutylene succinate blends,” *Polymer Bulletin* 79(7), 5481-5494.

<https://doi.org/10.1007/s00289-021-03567-3>

Article submitted: September 14, 2025; Peer review completed: November 22, 2025;

Revised version received: November 26, 2025; Accepted: November 30, 2025;

Published: December 15, 2025.

DOI: 10.15376/biores.21.1.1050-1064